Concurrent Induction of Antitumor Immunity and Autoimmune Thyroiditis in CD4$^+$CD25$^+$ Regulatory T Cell–Depleted Mice

Wei-Zen Wei,[1] Jennifer B. Jacob,[1,2] John F. Zielinski,[1] Jeffrey C. Flynn,[2] K. David Shim,[1] Ghazwan Alsharabi,[3] Alvaro A. Giraldo,[3] and Yi-chi M. Kong[2]

[1]Karmanos Cancer Institute and [2]Department of Immunology and Microbiology, School of Medicine, Wayne State University, and [3]Division of Immunopathology, St. John Hospital and Medical Center, Detroit, Michigan

Abstract

When CD4$^+$CD25$^+$ regulatory T cells are depleted or inactivated for the purpose of enhancing antitumor immunity, the risk of autoimmune disease may be significantly elevated because these regulatory T cells control both antitumor immunity and autoimmunity. To evaluate the relative benefit and risk of modulating CD4$^+$CD25$^+$ regulatory T cells, we established a new test system to measure simultaneously the immune reactivity to a tumor-associated antigen, neu, and an unrelated self-antigen, thyroglobulin. BALB/c mice were inoculated with TUBO cells expressing an activated rat neu and treated with anti-CD25 monoclonal antibody to deplete CD25$^+$ cells. The tumors grew, then regressed, and neu-specific antibodies and IFN-γ–secreting T cells were induced. The same mice were also exposed to mouse thyroglobulin by chronic i.v. injections. These mice produced thyroglobulin-specific antibody and IFN-γ–secreting T cells with inflammatory infiltration in the thyroids of some mice. The immune responses to neu or thyroglobulin were greater in mice undergoing TUBO tumor rejection and thyroglobulin injection than in those experiencing either alone. To the best of our knowledge, this is the first experimental system to assess the concurrent induction and possible synergy of immune reactivity to defined tumor and self-antigens following reduction of regulatory T cells. These results illustrate the importance of monitoring immune reactivity to self-antigens during cancer immunotherapy that involves immunomodulating agents, and the pressing need for novel strategies to induce antitumor immunity while minimizing autoimmunity. (Cancer Res 2005; 65(18): 8471-8)

Introduction

CD4$^+$CD25$^+$ regulatory T (Treg)–like cells have been described in patients with different types of cancers (1–3). We and others have shown that removal of CD4$^+$CD25$^+$ cells from tumor-bearing mice resulted in the regression of certain mouse tumors (4, 5), suggesting that Treg may negatively regulate antitumor immunity and depletion of Treg may be a powerful way to control tumor growth. In addition to CD4 and CD25, Treg express CTLA-4 (6), a glucocorticoid-induced tumor necrosis factor receptor family member (TNFRSF18; ref. 7), CD80 (8), CD62L, membrane-bound transforming growth factor β (9), as well as the transcription factor scurfin, encoded by *foxp3* (10). They do not proliferate when stimulated *in vitro* via CD3. Treg suppressive activity is triggered through the T-cell receptor by specific antigen and can inhibit T-cell activation in an antigen-specific (11) or nonspecific (12, 13) manner through a contact-dependent mechanism.

In this study, rat neu is used as the model tumor-associated antigen. Overexpression of erbB-2 or Her-2/neu in a number of common cancers, such as breast, ovarian, colorectal, prostate, and pancreatic adenocarcinoma (14–17), is correlated with a more aggressive course of disease (18, 19), rendering Her-2 an important target of cancer therapy. The therapeutic effect of anti–Her-2 monoclonal antibody (mAb), Herceptin, in stage IV breast cancer patients further distinguishes this molecule as an exceptional target of immunotherapy and vaccination. Because of self-tolerance, it is difficult to elicit strong immune responses to Her-2, as we showed in Her-2 transgenic mice (20), and Treg depletion may be a plausible strategy to amplify anti–Her-2/neu immunity.

Depletion of CD4$^+$CD25$^+$ cells combined with CTLA-4 blockade has been shown to enhance the efficacy of B16 melanoma cell vaccine with an increase in autoimmune skin depigmentation, demonstrating the concurrent induction of antitumor immunity and autoimmunity directed at common antigens (21). Autoimmunity induced through modulation of regulatory T cells is, however, not restricted to such common antigens. Autoimmune thyroiditis and a spectrum of other autoimmune diseases have been observed in cancer patients receiving melanoma gp100 or Her-2 peptide vaccines with immunomodulating agents (22, 23). In this study, we examined the induction of autoimmunity in the thyroid which does not share common antigens with Her-2.

We have shown that depletion of Treg in CBA/J mice increased their susceptibility to experimental autoimmune thyroiditis (24), the murine model of Hashimoto's thyroiditis. Hashimoto's thyroiditis, the leading cause of hypothyroidism, is characterized by mononuclear cell infiltration and destruction of the thyroid, elevation of thyroid-stimulating hormone, and decrease of thyroid hormones (T3 and T4). The production of autoantibodies (25) and T-cell proliferation to thyroid antigens (26) are indicators of autoreactivity. Susceptibility to thyroiditis is strongly influenced by the haplotype of class II MHC. For example, human *HLA-DRB1*0301* (DR3) transgene (27) and murine $H2^k$ (CBA/J) confer susceptibility to autoimmune thyroiditis, whereas murine $H2^d$ (BALB/c) is associated with resistance (28).

In genetically susceptible mice, experimental autoimmune thyroiditis is induced by injection of mouse thyroglobulin (mTg), usually in the presence of a strong adjuvant (e.g., complete Freund's Adjuvant or lipopolysaccharide; ref. 29), or by repeated injections of mTg for 4 weeks (30). Like Hashimoto's thyroiditis, experimental

Note: Supplementary data for this article are available at Cancer Research Online (http://cancerres.aacrjournals.org/).

Requests for reprints: Wei-Zen Wei, Karmanos Cancer Institute, Wayne State University, 110 East Warren Avenue, Detroit, MI 48201. Phone: 313-833-0715 Ext 2360; Fax: 313-831-7518; E-mail: weiw@karmanos.org.

©2005 American Association for Cancer Research.

doi:10.1158/0008-5472.CAN-05-0934

Downloaded from cancerres.aacrjournals.org on September 28, 2020. © 2005 American Association for Cancer Research.

autoimmune thyroiditis is also characterized by mononuclear cell infiltration, autoantibody production, and T-cell proliferation. Susceptible mice can be tolerized to mTg by short-term elevation of circulating mTg (31). This induced tolerance is abrogated by depletion of $CD25^+$ cells and mice again become susceptible to experimental autoimmune thyroiditis (24).

In this study, we assessed the risk of experimental autoimmune thyroiditis in genetically resistant BALB/c mice undergoing Treg depletion to induce tumor regression. Our results show that in a Treg-deprived environment, tumor cells effectively prime the immune system, resulting in tumor regression and persistent immunologic memory. The same depletion enhanced autoimmunity to mTg in resistant BALB/c mice. Concurrent tumor regression and mTg immunization resulted in further elevation of both antitumor and anti-mTg immunity. This report describes the first test system to analyze simultaneous antitumor and anti-self immunity while reducing immune regulatory mechanisms as a form of cancer therapy.

Materials and Methods

Mice and cell lines. Six- to eight-week-old female BALB/c mice ($H2^d$) were obtained from Charles River Laboratory (Frederick, MD). All animal procedures were conducted in accordance with accredited institution guidelines and the U.S. Public Health Service Policy on Humane Care and Use of Laboratory Animals (http://grants.nih.gov/grants/olaw/olaw.htm#pol). D2F2 is a mouse mammary tumor line derived from a spontaneous mammary tumor that arose in the BALB/c hyperplastic alveolar nodule line D2 (32). The TUBO cell line, kindly provided by Dr. Guido Forni (Department of Clinical and Biological Sciences, University of Turin, Orbassano, Italy), was derived from a spontaneous mammary tumor which arose in a BALB NeuT transgenic mouse expressing a transforming rat neu (33, 34). TUBO cells grow progressively in normal BALB/c mice and give rise to tumors which are histologically similar to those in BALB NeuT mice. All tissue culture reagents were purchased from Invitrogen (Carlsbad, CA) unless otherwise specified. Cell lines were maintained *in vitro* in DMEM supplemented with 5% heat-inactivated cosmic calf serum (Hyclone, Logan, UT), 5% heat-inactivated fetal bovine serum (Sigma, St. Louis, MO), 10% NCTC 109 medium, 2 mmol/L L-glutamine, 0.1 mmol/L MEM nonessential amino acids, 100 units/mL penicillin, and 100 μg/mL streptomycin. D2F2 cells were cotransfected with pRSV2/neo and pCMV/neu, which encodes wild-type rat *neu*. Stable clones of D2F2/neu were selected and the expression of neu protein on the cell surface was verified by flow cytometry. Transfected cell lines were maintained in medium containing 0.8 mg/mL G418 (Geneticin, Sigma).

Depletion of $CD25^+$ T cells with anti-CD25 monoclonal antibody, PC61. The hybridoma line PC61 which produces rat anti-mouse CD25 immunoglobulin G1 [IgG1; American Type Culture Collection (ATCC), Manassas, VA] was propagated in severe combined immunodeficient mice. BALB/c mice were injected i.p. with ~0.5 mg of PC61 or normal rat immunoglobulin (or PBS). Depletion of $CD25^+$ cells was verified by flow cytometry. Lymph node cells were prepared and washed with PBS containing 0.1% sodium azide and 2% cosmic calf serum. All samples were treated with Fc receptor blocker (rat antibody to CD16/CD32; PharMingen, San Diego, CA) for 15 minutes on ice, then washed once. Cells were incubated with goat anti-GITR IgG (R&D Systems, Minneapolis, MN) for 20 minutes on ice followed by allophycocyanin-rat anti-CD4 (RM4-5), FITC-rat anti-CD25 (7D4), and phycoerythrin-donkey anti-goat IgG. Controls were stained with FITC-rat immunoglobulin M, allophycocyanin-rat IgG2b, or normal goat IgG with phycoerythrin-donkey anti-goat IgG. mAb RM4-5, 7D4, and their isotype controls were from PharMingen. Normal goat IgG and phycoerythrin-donkey anti-goat IgG were from Jackson ImmunoResearch Lab (West Grove, PA). Single- and double-stained samples were used for instrument setup. Lymph node cells from naïve animals were measured in parallel. Flow cytometric analysis was done with a FACSCalibur (Becton Dickinson, Mountain View, CA).

Tumor growth and measurement. To measure tumor growth, mice were challenged s.c. with 2×10^5 cells in the flank. Tumor growth was monitored by weekly palpation. Tumor diameters were measured in two dimensions and mice were sacrificed when any one dimension reached 15 mm. Tumor volume was calculated as $X^2Y / 2$, where X and Y represent the short and long dimension, respectively, of the tumor. Comparison of tumor-free mice was analyzed with the log-rank test.

Measurement of anti-neu antibodies. Antibody response to rat neu was determined by flow cytometry as we previously described (35). BALB/c 3T3 cells (ATCC) were stably transfected with rat neu to establish 3T3/N cells. The mouse anti-rat neu mAb (IgG2a, clone 7.16.4), which recognizes an extracellular domain of rat neu protein (Oncogene Research Products, Cambridge, MA), was serially diluted and used to stain 3T3/N cells to establish a standard binding curve. FITC-goat anti-mouse IgG was the secondary antibody (Jackson ImmunoResearch). To determine antibody concentration in test sera, serially diluted test sera were used as primary antibody. Antibody concentration was calculated by regression analysis as we previously reported (35). Normal mouse immunoglobulin was used as negative control. The isotype of bound antibody was measured with FITC-goat anti-mouse IgG1 or IgG2a (Caltag, Burlingame, CA) and the results were expressed as mean channel fluorescence. Flow cytometric analysis was done with a FACSCalibur (Becton Dickinson). The results were analyzed by two-tailed Student's t test and are presented as mean ± SD.

Enumeration of cytokine-producing cells by ELISPOT assay. Spleen cells were suspended in RPMI 1640 supplemented with 10% FCS, 2 mmol/L L-glutamine, and 100 units/mL penicillin and 100 μg/mL streptomycin. Three to four hundred thousand cells were added to each well of the 96-well high-throughput screening immunoprecipitation plates (Millipore, Bedford, MA), which were precoated with rat anti-mouse IFN-γ (IgG1, clone R4-6A2) or rat anti-mouse interleukin 4 (IL-4; IgG1, clone 11B11), and incubated for 24 to 48 hours at 37°C in 5% CO_2. Test wells also contained the engineered antigen-presenting cells 3T3/NKB, which were 3T3 cells expressing rat neu, H2-K^d and CD80. The control 3T3/K cells were 3T3 cells expressing H2-K^d. The ratio of spleen cells to 3T3/NKB was 10:1 and 3T3/NKB were added after spleen cells had been plated. After incubation, cells were discarded and biotinylated rat anti–IFN-γ (IgG1, clone XMG 1.2) or rat anti–IL-4 (IgG1, clone BVD6-24G2) was added. All antibodies were purchased from BD PharMingen. Plates were incubated for 12 hours at 4°C, then washed to remove unbound antibody. Bound antibody was detected by incubating the plates with 0.9 μg/mL avidin-horseradish peroxidase (Sigma) for 2 hours at room temperature. Following washing, the substrate 3-amino-9-ethylcarbazole in 0.1 mol/L acetic acid and 0.003% hydrogen peroxide was added and the plates were incubated for 5 minutes. The substrate was discarded and the plates were washed six times with water. The visualized cytokine spots were enumerated with the ImmunoSpot analyzer (CTL, Cleveland, OH) and the results expressed as the number of cytokine-producing cells per 10^6 spleen cells. Data were analyzed by Student's t test.

Immunization with mouse thyroglobulin. mTg was prepared from frozen thyroids by fractionation on a Sephadex G-200 column as previously described (36, 37) and diluted in nonpyrogenic saline before use. The presence of lipopolysaccharide was measured by *Limulus* amoebocyte assay (Associates of Cape Cod, Woods Hole, MA; ref. 30). A 40 μg dose of mTg contained <0.5 ng of lipopolysaccharide.

Mice were injected i.v. with 40 μg mTg, followed in 3 hours with 20 μg *Salmonella enteritidis* lipopolysaccharide. The injections were repeated in 7 days. Alternatively, 40 μg mTg was injected i.v. on 4 successive days with 3 days of rest (30). This treatment was repeated for 3 more weeks.

Measurement of anti–mouse thyroglobulin antibody. Anti-mTg antibody titers were determined by ELISA as previously described (38). Briefly, Immulon I microtiter plates (Dynatech Laboratories, Inc., Chantilly, VA) were coated with mTg at 1 μg/well and serially diluted test sera were added. After washing, bound antibody was detected with alkaline phosphatase–labeled goat anti-mouse IgG and enzyme substrate.

Measurement of anti–mouse thyroglobulin T-cell response. T-cell proliferation was measured by [^{3}H]thymidine incorporation. Splenocytes were cultured in triplicate in RPMI + 1% normal mouse serum, 2 mmol/L L-glutamine, 5×10^{-5} mol/L β-mercaptoethanol, 100 units/mL penicillin,

Downloaded from cancerres.aacrjournals.org on September 28, 2020. © 2005 American Association for Cancer Research.

and 100 μg/mL streptomycin, in 96-well plates at 6×10^5 cells/well, either with or without 40 μg/mL mTg for 4 days at 37°C, 6% CO_2. The cells were pulsed with 1.2 μCi/well of [^{3}H]thymidine and incubated for 18 hours before harvest onto glass fiber filter paper (Tomtec Mach3Man Cell Harvester, LKB Wallac, Gaithersburg, MD). [^{3}H]Thymidine was measured with a Microbeta Plus 1450 liquid scintillation counter (LKB Wallac). Data were analyzed by two-tailed Student's *t* test.

IFN-γ– and IL-4–producing cells were enumerated by ELISPOT assay using 40 μg/mL mTg as the antigen. In some experiments, a two-step ELISPOT assay was done to amplify mTg-specific T-cell response. Spleen cells and mTg were incubated in 96-well tissue culture plates for 3 days before the content of the wells was transferred to high-throughput screening immunoprecipitation plates. The high-throughput screening immunoprecipitation plates were incubated for 24 hours. The detection and enumeration of cytokine spots was done as described earlier.

Histologic evaluation of experimental autoimmune thyroiditis. Thyroid specimens were sectioned vertically through both lobes and 50 to 60 histologic sections were prepared from 10 to 15 step levels. The extent of mononuclear cell infiltration was scored based on the pathology index scale of 0 to 4 and presented as percent thyroid infiltration: 0, no infiltration; 0.5, >0% to 10% thyroid infiltration consisting of perivascular foci without follicular destruction; 1.0, >10% to 20% thyroid infiltration with follicular destruction; 2.0, >20% to 40% diffuse thyroid infiltration; 3.0, >40% to 80% thyroid destruction; and 4.0, >80% to 100% thyroid destruction (36). The sections were scored without knowledge of the groups. Statistical differences were analyzed by the nonparametric Mann-Whitney *U* test.

Statistical analyses. Tumor growth expressed as percent tumor-free mice was analyzed with the log-rank test. Thyroiditis expressed as percent infiltration of thyroid was analyzed using the nonparametric Mann-Whitney *U* test. The number of IFN-γ–producing cells and the antibody levels were analyzed by Student's *t* test.

Results

Duration of CD4$^+$CD25$^+$GITR$^+$ T-cell depletion by anti-CD25 monoclonal antibody treatment. To establish the time window of Treg depletion by anti-CD25 mAb, BALB/c mice were injected i.p. on 2 consecutive days with 0.5 mg of anti-CD25 mAb, PC61. CD4$^+$CD25$^+$GITR$^+$ T cells in the lymph nodes were enumerated on days 0 to 12 after the second injection. On each test day, three test mice were sacrificed and their lymph node cells analyzed individually. Control cells were prepared by pooling lymph node cells from three mice which received normal rat immunoglobulin or PBS. Cells were stained with allophycocyanin-anti-CD4, FITC-anti-CD25, and goat anti-GITR with phycoerythrin-conjugated secondary antibodies and analyzed by flow cytometry. Figure 1 shows representative T-cell profiles on days 0, 3, 5, 9, and 12. CD4$^+$ T cells were gated (Fig. 1*A*) and percentages of CD25$^+$GITR$^+$ cells in gated CD4$^+$ cells are shown in density plots (Fig. 1*B*). The results from all test and control mice are summarized in a table and provided in the Supplementary data. In CD4$^+$ T cells, the majority of CD25$^+$ cells were also GITR^{hi}. These triple-positive cells were reduced from 11 ± 0.1% to 6.2% ± 0.5% on day 1, reached their nadir of 3.0 ± 0.7% by day 5, and began to reappear after day 9. Therefore, treatment with anti-CD25 mAb maximally reduced CD4$^+$CD25$^+$GITR$^+$ cells between days 5 and 7.

TUBO tumor regression in Treg-depleted mice. *In vivo* priming to tumor-associated antigens after Treg depletion was tested with TUBO tumor, which was established from a spontaneous mammary tumor in BALB NeuT mice expressing a transforming rat neu (33, 34). Consequently, TUBO cells express neu on their cell surface (Fig. 2*A, inset*). Anti-CD25 mAb was administered twice, either 5 and 6 days before or 1 and 3 days after tumor cell inoculation. In naïve mice, TUBO tumors grew progressively to reach >500 mm^3 (not shown) when mice were sacrificed. In anti-CD25 mAb–treated mice, all mice developed tumors which started to regress when they were 15 to 180 mm^3 in size, and regressed completely by week 11 (Fig. 2*A*), suggesting *in vivo* priming by a growing TUBO tumor. The course of tumor growth and regression was nearly identical whether anti-CD25 mAb was administered before or after tumor cell inoculation. This experiment was repeated at least twice with similar results.

Anti-neu immunity in mice undergoing TUBO tumor regression. To characterize the immune responses induced during TUBO tumor regression, sera were collected at 5 and 9 weeks following tumor cell inoculation and anti-neu antibody was measured by flow cytometry as we previously reported (35). As shown in Fig. 2*B*, in naïve mice, tumor growth did not induce detectable anti-neu antibody at week 5. The tumor volume exceeded 500 mm^3 at week 9 (not shown), at which time 11.4 ± 3.5 μg/mL of anti-neu IgG was detected. Mice treated with anti-CD25 mAb before and after tumor cell inoculation displayed 11.7 ± 8.6 and 8.9 ± 6.4 μg/mL, respectively, of anti-neu IgG at week 5, when the tumors were ~35 mm^3. At week 9, when the tumors were almost completely eliminated, these same mice had 16.7 ± 9 and 34 ± 9 μg/mL of anti-neu IgG, respectively (P = 0.01). Thus, depletion of CD25$^+$ T cells either before or after TUBO cell inoculation resulted in a more prompt and elevated antibody response, with the highest level of anti-neu IgG observed at week 9 in mice receiving anti-CD25 after TUBO cell inoculation (Fig. 2*B*). The isotypes of antibodies were further analyzed. Figure 2*C* shows the representative week 5 results from mice treated with α-CD25 before tumor inoculation. Both IgG1 and IgG2a were elevated, suggesting activation of both T-helper (Th) 1 and Th2 cells.

To measure neu-specific T-cell response, four tumor-free mice which received anti-CD25 after TUBO cell inoculation were sacrificed at week 9. Their spleen cells were isolated and incubated individually with the engineered 3T3/NKB cells. IFN-γ– and IL-4–producing cells were enumerated by ELISPOT assay after a 2-day culture and similar results were obtained from the four mice. Figure 2*D* shows the result from a representative animal. There were 36 ± 2

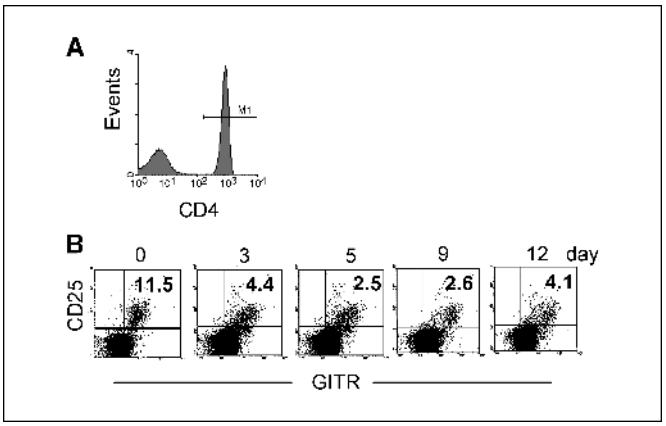

Figure 1. Depletion of Treg with anti-CD25 mAb PC61. BALB/c mice were injected i.p. with 0.5 mg of anti-CD25 mAb on 2 consecutive days. Lymph node cells were collected from treated and control mice on days 0, 1, 3, 5, 9, and 12 after antibody treatment. The cells were stained with allophycocyanin-anti-CD4, FITC-anti-CD25, and goat anti-GITR with phycoerythrin-anti-goat IgG. Positively stained CD4$^+$ T cells were gated (*A*) and CD25 and GITR profiles of gated CD4$^+$ cells harvested on days 0, 3, 5, 9, and 12 were depicted as dot plots (*B*). The number in the top right quadrant represents the percentage of CD25$^+$GITR$^+$ cells within the CD4$^+$ T-cell population.

Downloaded from cancerres.aacrjournals.org on September 28, 2020. © 2005 American Association for Cancer Research.

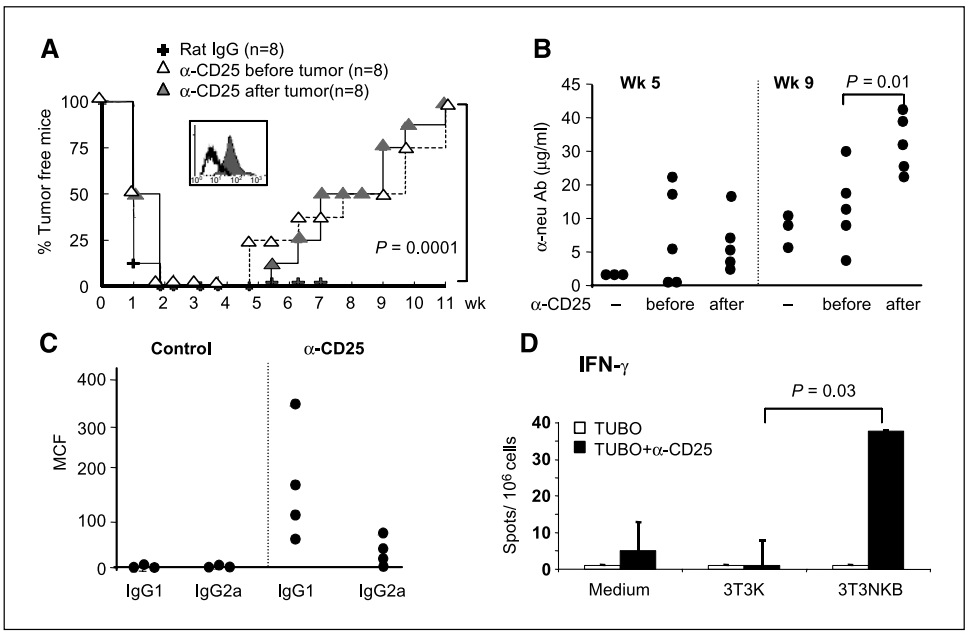

Figure 2. Tumor regression following Treg depletion. BALB/c mice were injected i.p with 0.5 mg anti-CD25 mAb either 5 and 6 days before or 1 and 3 days after they received 2×10^5 TUBO cells. Control mice were treated with normal rat immunoglobulin or PBS. There were eight mice in each group. Tumor growth was monitored for 11 weeks. *A,* TUBO tumor growth in mice treated with anti-CD25 before (△) or after (▲) tumor cell inoculation or in control mice (+). The results are expressed as percentage of tumor-free mice. *Inset,* expression of neu on TUBO cells was verified by flow cytometry using mouse anti-rat neu mAb (7.16.4, *filled histogram*) followed by phycoerythrin-anti-mouse immunoglobulin, and compared with isotype controls (*open histogram*). *B,* anti-neu IgG levels in mice treated with anti-CD25 before or after TUBO cell inoculation were measured by flow cytometry and calculated by regression analysis. *C,* IgG1 and IgG2a levels in mice treated with anti-CD25 mAb after TUBO cell inoculation are reported as mean channel fluorescence (*MCF*). *D,* T-cell response to neu antigen. Following anti-CD25 mAb treatment and tumor regression, tumor-free mice were sacrificed at week 9 and their spleen cells isolated and cultured with 3T3/K or 3T3/NKB cells. IFN-γ–producing cells were enumerated by ELISPOT assay, and normalized to express the number of spots per 10^6 spleen cells.

neu-specific IFN-γ–producing cells per 10^6 spleen cells. Neu-specific IL-4–producing cells were not detected (not shown), suggesting a more prominent Th1 response. Stimulation with concanavalin A typically resulted in over 1,000 spots per 10^6 spleen cells (not shown). Incubation with 3T3/K cells did not induce IFN-γ or IL-4 production.

Immunologic memory to tumor-associated antigen. To assess the strength of immunologic memory to tumor-associated antigens, the group of eight mice which rejected TUBO tumors by anti-CD25 mAb treatment postinoculation were rechallenged with TUBO or D2F2/neu cells at week 14 (week 0 in Fig. 3*A*). TUBO tumors were rejected by all three mice receiving this cell line as the second challenge (Fig. 3*A*). The other five mice received D2F2/neu cells, which were generated by transfecting a prolactin-induced BALB/c mammary tumor D2F2 with the wild-type rat neu (Fig. 3*B*; ref. 39). D2F2/neu cells were rejected by 4 of 5 (80%) mice. Mice which rejected TUBO tumors had 34 ± 9 μg/mL anti-neu antibody just before they received the second tumor challenge. The level of antibody cross-reactive with D2F2 was below 1 μg/mL and remained low after these mice rejected D2F2/neu, suggesting that the second challenge of D2F2/neu cells was rejected primarily through anti-neu immunity.

In summary, depletion of Treg in mice carrying TUBO tumors resulted in anti-neu antibodies, neu-specific IFN-γ–producing T cells, eradication of the growing tumor, as well as immunologic memory to neu and possibly other tumor-associated antigens.

Experimental autoimmune thyroiditis induced in resistant BALB/c mice. We have shown that elimination of Treg in mTg-tolerized CBA/J mice resulted in their reversion to the susceptible phenotype (4, 24). To test whether depletion of Treg in BALB/c mice, an experimental autoimmune thyroiditis–resistant mouse strain, would render them susceptible, mice were treated with anti-CD25 mAb twice, 4 days apart. On days 5 and 12 after the second mAb injection, mice received 40 μg of mTg and 20 μg of lipopolysaccharide (29), and they were sacrificed 4 weeks after the second immunization. Anti-mTg antibody was measured by ELISA. Depletion of Treg before mTg and lipopolysaccharide treatment resulted in a significant increase in anti-mTg antibodies ($P = 0.003$; Fig. 4*A*), including both IgG1 and IgG2a. To measure T-cell response, splenocytes were cultured with mTg for 4 days and cell proliferation was measured by [^{3}H]thymidine incorporation. A significant increase ($P = 0.002$) in T-cell response was detected in mice depleted of Treg (Fig. 4*B*). The incidence and severity of thyroiditis was significantly increased ($P = 0.01$) with Treg depletion (Fig. 4*C*). Compared with control mice without anti-CD25 mAb treatment,

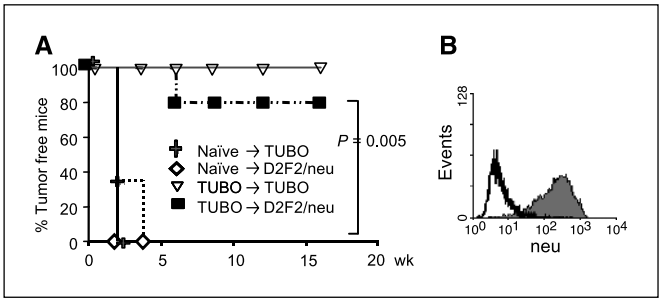

Figure 3. Induction of memory T cells after Treg depletion and tumor regression. *A,* BALB/c mice which had been treated with anti-CD25 at 1 and 3 days following TUBO cell inoculation, and of which tumors had regressed, were rechallenged with 2×10^5 TUBO or D2F2/neu cells. Three mice were given a second challenge with TUBO (▽) and five mice with D2F2/neu tumor cells (■). Control groups were naïve mice inoculated with D2F2/neu (◇) or TUBO (+) cells. *B,* flow cytometric analysis of D2F2/neu cells (*filled histogram*). Normal mouse immunoglobulin was used as control (*open histogram*).

Downloaded from cancerres.aacrjournals.org on September 28, 2020. © 2005 American Association for Cancer Research.

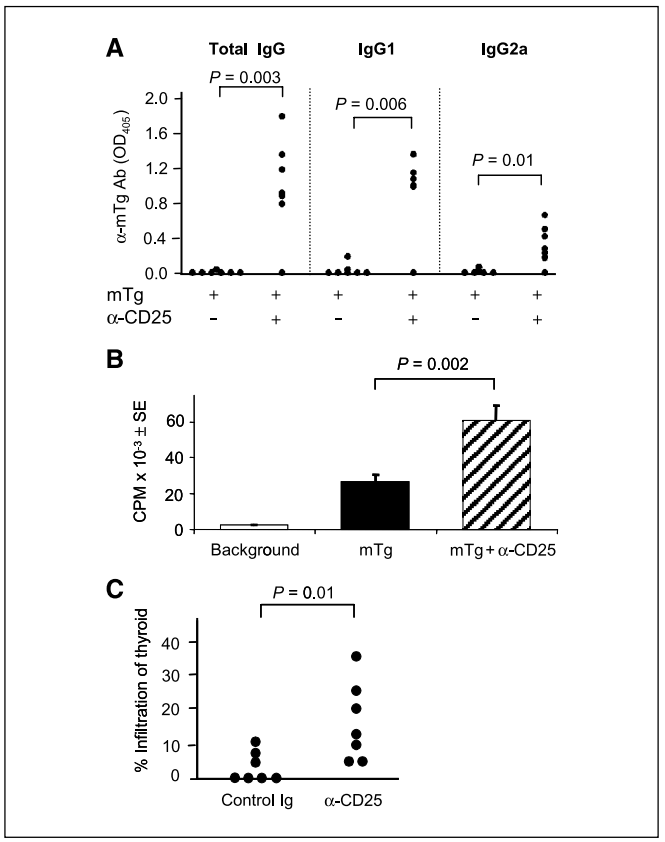

Figure 4. Enhanced anti-mTg immunity following Treg depletion. BALB/c mice were injected with 0.5 mg anti-CD25 mAb 4 days apart. On days 5 and 12 after the second injection, each mouse received i.v. 40 μg mTg and 20 μg lipopolysaccharide. On day 40, thyroids, sera, and spleen cells were collected for evaluation. *A,* mTg antibody measured by ELISA. Serum samples were tested at 1:2,500 dilution. *B, in vitro* proliferative response to mTg. A total of 6×10^5 spleen cells were incubated in the presence of 40 μg/mL mTg for 4 days and [^{3}H]thymidine uptake was measured. *C,* infiltration of individual thyroids by mononuclear cells in histologic sections was recorded. There were seven mice in each group.

the incidence of thyroid infiltration was 100% (7 of 7) versus 43% (3 of 7). Follicular destruction which is associated with >10% mononuclear infiltration of the thyroid was detected only in Treg-depleted mice. Therefore, removal of Treg enabled "resistant" BALB/c mice to develop moderate experimental autoimmune thyroiditis.

Concurrent induction of anti-neu and anti–mouse thyroglobulin response in Treg-depleted mice. To evaluate the risk of autoimmunity in mice undergoing Treg depletion to enhance antitumor immunity, we inoculated BALB/c mice with TUBO cells, followed on days 1 and 3 with anti-CD25 mAb (Fig. 5*A*). The same mice also received mTg to assess the concurrent induction of anti-mTg immunity. Rather than immunizing with mTg and lipopolysaccharide, because the latter may complicate antitumor immunity, mice received 40 μg of mTg i.v. on 4 consecutive days each week, for 4 weeks. In our previous report, this regimen induced experimental autoimmune thyroiditis in about 50% of susceptible CBA/J mice (30). All mice inoculated with tumor cells developed solid tumors in 2 weeks (Fig. 5*A* and *B*). In naïve mice, the tumors grew progressively and mice were sacrificed by week 7. All mice receiving TUBO cells and mTg without Treg depletion developed tumors by week 3. None of the tumors regressed (Fig. 5*A* and *B*). In mice depleted of Treg, tumors started to regress when they reached ~100 mm^3 and three of four tumors regressed completely. In all seven mice which received anti-CD25 mAb and mTg, TUBO tumors completely regressed. A repeated experiment showed similar results. Therefore, TUBO tumors were rejected following Treg depletion regardless of the presence of mTg.

To characterize the immune response, anti-neu antibodies were measured at week 10 or at time of sacrifice. Anti-neu IgG in untreated, tumor-bearing mice averaged 6 ± 2.4 μg/mL (Fig. 5*C*). With Treg depletion and tumor regression, average antibody level increased to 28.7 ± 26 μg/mL. Although the difference did not reach statistical significance, an increase in anti-neu antibody was observed consistently after Treg depletion. Serum samples from these two groups did not react with mTg when tested by ELISA (not shown), showing the absence of cross-reactivity between neu and mTg. Interestingly, exposure to mTg in Treg-depleted mice which undergo TUBO tumor regression resulted in an average of 78.6 ± 56 μg/mL of anti-neu IgG, demonstrating an up-regulation of anti-neu response in about 50% of the mice responding to both neu and mTg ($P = 0.05$). Neu-specific T-cell response was measured by ELISPOT following *in vitro* stimulation with the engineered antigen-presenting cells 3T3/NKB. Low, but detectable, IFN-γ–producing cells were detected following tumor regression. Figure 5*D* shows the result of a representative experiment from four independent analyses. Reactive T cells increased to ~45 per 10^6 spleen cells after the mice were also immunized with mTg. Neu-specific IL-4–producing cells were not detected (not shown). Therefore, injection of mTg in TUBO cell–bearing mice without anti-CD25 mAb treatment did not result in enhanced anti-neu immunity (Fig. 5*C* and *D*), demonstrating that exposure to mTg, a self-antigen, per se did not enhance antitumor immunity. Rather, depletion of regulatory T cells resulted in tumor regression with anti-neu immunity, which is further enhanced when anti-mTg reactivity is also triggered with this regimen.

To assess anti-mTg response in Treg-depleted mice which received mTg immunization after TUBO cell inoculation, serum antibody to mTg was measured. In three of seven mice, the antibody level was higher than that in mice which were immunized with mTg after Treg depletion, but were not inoculated with tumor cells, although the difference between these two groups was not statistically significant with this sample size (Fig. 6*A*). Mice inoculated with TUBO cells and treated with anti-CD25 mAb did not produce anti-mTg antibody. Anti-mTg antibody in Treg-depleted, mTg-immunized mice did not interact with neu when measured by flow cytometry (not shown), showing the absence of cross-reactivity between mTg and neu. mTg-specific T-cell proliferation or cytokine production was not detected at week 9 (not shown). To amplify possible T-cell responses, spleen cells were cultured with mTg for 3 days before they were transferred to ELISPOT plates precoated with anti–IFN-γ (Fig. 6*B*) or anti–IL-4 (Fig. 6*C*). Using this two-step ELISPOT assay, 612 ± 31 IFN-γ–producing and 79 ± 10 IL-4–producing cells per 10^6 spleen cells were detected in Treg-depleted mice which received TUBO and mTg. Mice inoculated with TUBO cells and injected with mTg did not develop T-cell response to mTg (not shown). Histologic analysis of the thyroid glands revealed low level of mononuclear cell infiltration, consisting mostly of T lymphocytes and macrophages as we previously reported (36, 40), in 3 of 7 mice (43%; Fig. 6*D*). Photomicrograph showing an area of thyroid with mononuclear cell infiltration is shown in Fig. 6*E*. There were no pathologic changes in thyroids of mice which received mTg without experiencing tumor. Therefore, depletion of Treg enhanced autoreactivity to mTg with further elevation after tumor regression, leading to thyroid infiltration.

Downloaded from cancerres.aacrjournals.org on September 28, 2020. © 2005 American Association for Cancer Research.

Discussion

The observed tumor regression in Treg-depleted mice was paralleled by the induction of anti-neu immunity. The accelerated and heightened anti-neu antibody response may contribute significantly to TUBO tumor regression because BALB NeuT tumors, like TUBO, are effectively controlled by anti-neu antibody (41). This may be due to antibody-mediated down-regulation of neu protein and neu-mediated signaling, which is critical to their survival. Antibody-dependent, cell-mediated cytotoxicity may also contribute to tumor destruction. Significant anti-neu T-cell response was shown. Unlike TUBO cells, the rejection of D2F2/neu cells is controlled primarily by T cells as we previously described (42, 43). Rejection of D2F2/neu supports the presence of neu-specific memory T cells after TUBO tumor regression. Therefore, both humoral and cellular immune responses to tumor-associated antigen were significantly elevated following Treg depletion.

Anti-neu and anti-mTg IgG1 and IgG2a were detected in Treg-depleted mice, suggesting the activation of both Th1 and Th2 cells. When T-cell response was tested, neu-specific IFN-γ–producing cells, but not IL-4–producing cells, were detected. mTg-specific IFN-γ– and IL-4–producing T cells were detected in the amplified two-step ELISPOT assay with greater number in IFN-γ–producing cells. These results show that depletion of Treg enhanced both Th1 and Th2 immunity.

T-cell response to mTg is usually evaluated by [^{3}H]thymidine incorporation because, unlike anti-mTg antibody response, *in vitro* proliferation generally correlates with thyroid infiltration (36). Compared with T-cell proliferation, ELISPOT assay for IFN-γ–producing cells is more sensitive in detecting T-cell response. It is possible to further amplify the sensitivity of ELISPOT assay by the two-step incubation. Immune cells were expanded by preculturing with the antigen for 3 days before they were subjected to ELISPOT assay. If we estimate that effector cells divide every 12 to 16 hours on antigen stimulation, the cell number would increase between 16- and 64-fold in 3 days. Every 16 to 64 spots detected in the amplified ELISPOT assay would represent one responding cell in the starting population. The sensitivity of ELISPOT is increased significantly by preincubation, yet the difference between the control and test groups is unequivocal.

Induction of experimental autoimmune thyroiditis in Treg-depleted BALB/c mice indicated that resistance to experimental autoimmune thyroiditis determined by MHC class II was influenced in part by Treg because mononuclear cell infiltration was much less pronounced in resistant BALB/c mice carrying intact Treg (Fig. 4*C*). After depletion, greater humoral and cellular immunity to mTg was induced by the conventional immunization with mTg and lipopolysaccharide (Fig. 4*A* and *B*). When immunized by repeated mTg injection without lipopolysaccharide as adjuvant, a mild response to mTg was induced, but the response was significantly elevated in mice undergoing tumor regression such that more mice developed inflammatory infiltration in their thyroids (Fig. 6*D*). The mononuclear cell infiltration of ~10% in this experiment was insufficient to cause thyroid hormonal changes. Nevertheless, this synergy between anti-neu and anti-mTg responses was both intriguing and alarming. Although the specific mechanisms remain to be delineated, it is possible that repeated injections of the self-antigen mTg in Treg-depleted mice not only stimulated mTg-specific T cells, but that the attendant inflammatory cytokines released systemically may also enhance antitumor response. From the tumor standpoint, in Treg-depleted mice, TUBO tumors grew to palpable size before sufficient immune effectors were generated to commence tumor regression. At the tumor site, tumor cell destruction can be envisioned following immunologic attack.

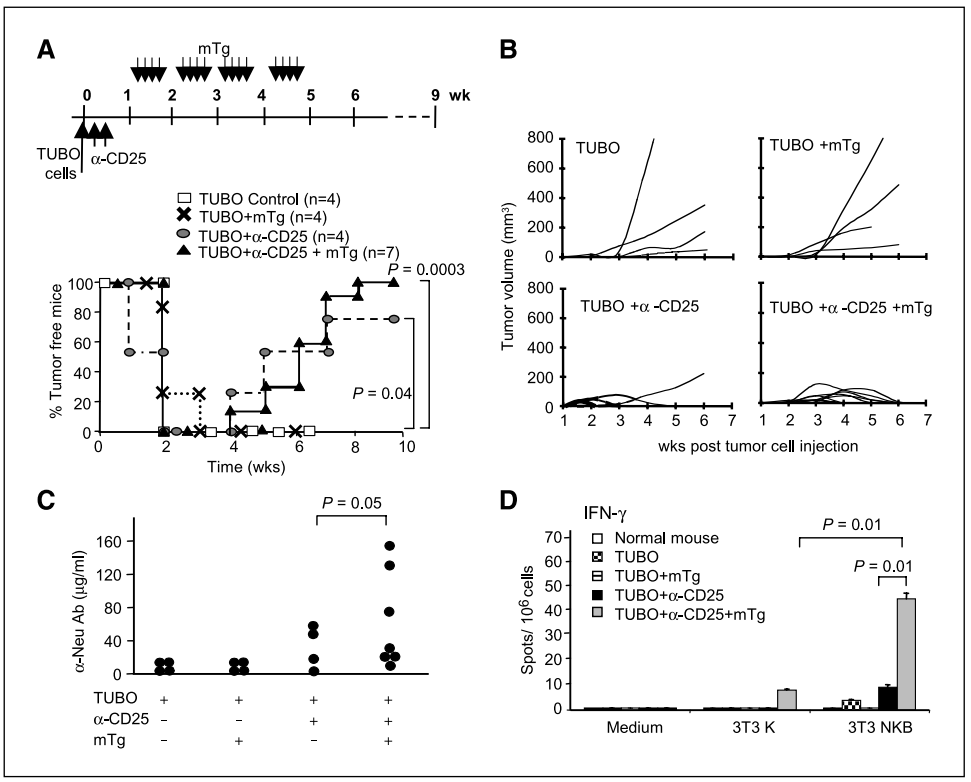

Figure 5. Effect of Treg depletion and mTg immunization on anti-neu immunity in TUBO cell–inoculated mice. BALB/c mice were inoculated with TUBO cells on day 0 and treated with anti-CD25 mAb on days 1 and 3. Starting on day 10 and continuing for 4 weeks, mice were injected with 40 μg of mTg daily for 4 days followed by a 3-day rest before the next cycle of injections. There were three other groups of mice which received TUBO cells and anti-CD25 mAb or mTg immunization or untreated. *A,* tumor growth in Treg-depleted mice with (▲) or without (●) mTg treatment. Mice in the control group received PBS (□) or mTg (×). *B,* tumor volume of individual mice in *A*. *C,* at week 10, anti-neu antibody was measured by flow cytometry; *D,* IFN-γ–producing cells were analyzed by ELISPOT assay. There were four mice in each group except seven mice in the group receiving TUBO cells, anti-CD25, and mTg.

Downloaded from cancerres.aacrjournals.org on September 28, 2020. © 2005 American Association for Cancer Research.

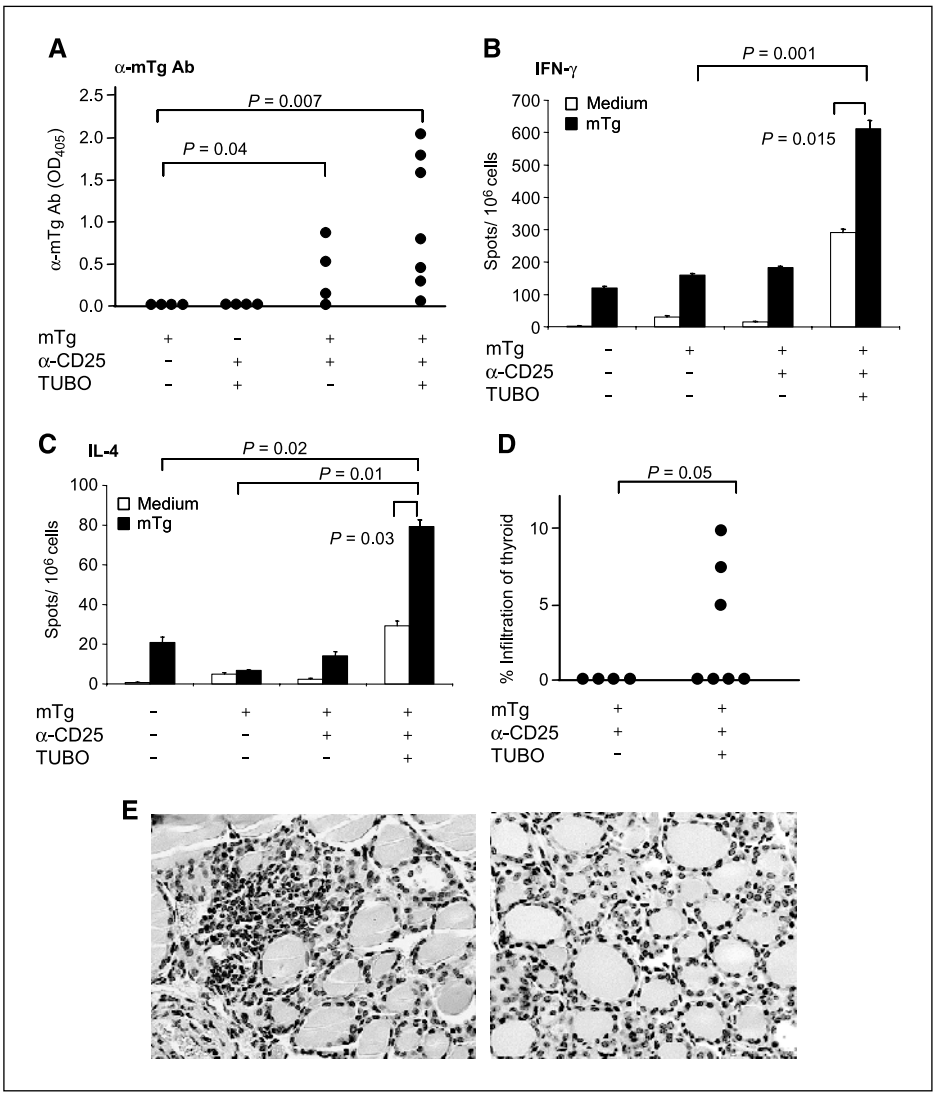

Figure 6. Effect of Treg depletion and TUBO tumor regression on anti-mTg immunity. There were four groups of mice; two groups were the same mice as described in Fig. 5 (i.e., mice injected with TUBO cells, treated with anti-CD25, and immunized with mTg, and the control mice). There were two additional groups of mice receiving mTg with or without anti-CD25, but not inoculated with TUBO cells. *A,* serum samples were diluted 1:2,500 and anti-mTg IgG measured by ELISA. IFN-γ–producing (*B*) and IL-4–producing (*C*) T cells were determined by the two-step ELISPOT assay. *D,* infiltration of individual thyroids by mononuclear cells was recorded. *E,* photomicrographs showing a normal thyroid section from an untreated mouse (*right*) and mononuclear cell infiltration with thyroid follicular destruction involving >10% of the thyroid from a Treg-depleted mouse which experienced TUBO tumor regression and mTg immunization (*left*); original magnification, ×200.

A cascade of immunologic events may lead to elevated reactivity to both mTg and tumor-associated antigens.

In cancer patients, more strenuous effort than one-time depletion may be required to overcome immune regulatory mechanisms before effective antitumor immunity can be induced, with increasing risk of autoimmunity from each new regimen. Our results showed that even genetically resistant BALB/c mice became more susceptible to experimental autoimmune thyroiditis once Treg were removed, particularly during tumor regression. Patients expressing high-risk *HLA* haplotypes will require close monitoring of their autoreactivity to self-antigens when their immune regulatory mechanisms are modulated. In a pilot study to test Her-2 peptide vaccine with Flt3 ligand administered systemically as an adjuvant, 2 of 15 subjects developed elevated thyroid stimulating hormone with symptoms of grade 2 hypothyroidism, indicating thyroid destruction. Thyroid hormone replacement therapy was required at the conclusion of the study (22). Significantly elevated levels of antibody to thyroglobulin and thyroid peroxidase were detected in one patient, demonstrating autoimmunity to thyroid antigens. In another study, 14 patients with metastatic melanoma received gp100 peptide vaccines along with mAb to CTLA-4, which is expressed on regulatory and activated T cells (23). In six patients, grade III/IV autoimmune manifestations were observed, including dermatitis, enterocolitis, hepatitis, and hypophysitis. The three patients with objective cancer regression all developed severe autoimmune symptoms requiring treatment. Because of the grade III/IV autoimmune toxicity in ≥3 patients, accrual intended for 21 patients ceased after 14 patients were enrolled. Therefore, immunomodulating reagents which can amplify antitumor immunity in a profound manner can trigger significant autoimmunity to self-antigens. For patients with genetic predisposition, the risk of autoimmunity may be overwhelming. With the sensitive *in vitro* assays to monitor immune reactivity to self-antigens, it may be possible to detect the onset of autoimmunity during cancer immunotherapy before clinical symptoms and counter measures may be taken in a timely fashion.

Acknowledgments

Received 3/21/2005; revised 6/2/2005; accepted 7/11/2005.

Grant support: NIH grants CA 76340 (W-Z. Wei) and DK45960 (Y.M. Kong), grant W81XWH-04-1-0546 from the Department of Defense (W-Z. Wei), and grant from St. John Hospital and Medical Center (Y.M. Kong).

The costs of publication of this article were defrayed in part by the payment of page charges. This article must therefore be hereby marked *advertisement* in accordance with 18 U.S.C. Section 1734 solely to indicate this fact.

Downloaded from cancerres.aacrjournals.org on September 28, 2020. © 2005 American Association for Cancer Research.

References

1. Curiel TJ, Coukos G, Zou L, et al. Specific recruitment of regulatory T cells in ovarian carcinoma fosters immune privilege and predicts reduced survival. Nat Med 2004;10:942–9.
2. Woo EY, Yeh H, Chu CS, et al. Regulatory T cells from lung cancer patients directly inhibit autologous T cell proliferation. J Immunol 2002;168:4272–6.
3. Viguier M, Lemaitre F, Verola O, et al. Foxp3 expressing CD4+CD25(high) regulatory T cells are overrepresented in human metastatic melanoma lymph nodes and inhibit the function of infiltrating T cells. J Immunol 2004;173:1444–53.
4. Wei WZ, Morris GP, Kong YM. Anti-tumor immunity and autoimmunity: a balancing act of regulatory T cells. Cancer Immunol Immunother 2004;53:73–8.
5. Jones E, Dahm-Vicker M, Simon AK, et al. Depletion of CD25+ regulatory cells results in suppression of melanoma growth and induction of autoreactivity in mice. Cancer Immun 2002;2:1–12.
6. Read S, Malmstrom V, Powrie F. Cytotoxic T lymphocyte-associated Antigen 4 plays an essential role in the function of CD25+CD4+ regulatory cells that control intestinal inflammation. J Exp Med 2000;192: 295–302.
7. Shimizu J, Yamazaki S, Takahashi T, Ishida Y, Sakaguchi S, Aavik E. Stimulation of CD25+CD4+ regulatory T cells through GITR breaks immunological self-tolerance. Nat Immunol 2002;3:135–42.
8. Salomon B, Lenschow DJ, Rhee L, et al. B7/CD28 costimulation is essential for the homeostasis of the CD4+CD25+ immunoregulatory T cells that control autoimmune diabetes. Immunity 2000;12:431–40.
9. Nakamura K, Kitani A, Striber W. Cell contact-dependent immunosuppression by CD4+ CD25+ regulatory T cells is mediated by cell surface-bound transforming growth factor β. J Exp Med 2001;194: 629–44.
10. Hori S, Nomura T, Sakaguchi S. Control of regulatory T cell development by the transcription factor Foxp3. Science 2003;299:1057–61.
11. Tanchot C, Vasseur F, Pontoux C, Garcia C, Sarukhan A. Immune regulation by self-reactive T cells is antigen specific. J Immunol 2004;172:4285–91.
12. Sakaguchi S. Control of immune responses by naturally arising CD4+ regulatory T cells that express toll-like receptors. J Exp Med 2003;197:397–401.
13. Gallimore A, Sakaguchi S. Regulation of tumour immunity by CD25+ T cells. Immunol 2002;107:5–9.
14. Slamon DJ, Godolphin W, Jones LA, et al. Studies of the HER-2/neu proto-oncogene in human breast and ovarian cancer. Science 1989;244:707–12.
15. Yu D, Hung MC. Overexpression of ErbB2 in cancer and ErbB2-targeting strategies. Oncogene 2000;19: 6115–21.
16. Tzahar E, Yarden Y. The ErbB-2/HER2 oncogenic receptor of adenocarcinomas: from orphanhood to multiple stromal ligands. Biochim Biophys Acta 1998;1377:M25–37.
17. Baxevanis CN, Sotiropoulou PA, Sotiriadou NN, Papamichail M. Immunobiology of HER-2/neu oncoprotein and its potential application in cancer immunotherapy. Cancer Immunol Immunother 2004; 53:166–75.
18. Gullick WJ, Love SB, Wright C, et al. c-erbB-2 protein overexpression in breast cancer is a risk factor in patients with involved and uninvolved lymph nodes. Br J Cancer 1991;63:434–8.
19. Menard S, Pupa SM, Campiglio M, Tagliabue E. Biologic and therapeutic role of Her-2 in cancer. Oncogene 2003;22:6570–8.
20. Piechocki MP, Ho YS, Pilon S, Wei WZ. Human ErbB-2 (Her-2) transgenic mice: a model system for testing Her-2 based vaccines. J Immunol 2003;171:5787–94.
21. Sutmuller RPM, van Duivenvoorde LM, van Elsas A, et al. Synergism of cytotoxic T lymphocyte-associated antigen 4 blockade and depletion of CD25+ regulatory T cells in antitumor therapy reveals alternative pathways for suppression of autoreactive cytotoxic T lymphocyte responses. J Exp Med 2001;194:823–32.
22. McNeel DG, Knutson KL, Schiffman K, Davis DR, Caron D, Disis ML. Pilot study of an HLA-A2 peptide vaccine using flt3 ligand as a systemic vaccine adjuvant. J Clin Immunol 2003;23:62–72.
23. Phan GQ, Yang JC, Sherry RM, et al. Cancer regression and autoimmunity induced by cytotoxic T lymphocyte-associated antigen 4 blockade in patients with metastatic melanoma. Proc Natl Acad Sci U S A 2003;100:8372–7.
24. Morris GP, Chen L, Kong YM. CD137 signaling interferes with activation and function of CD4+CD25+ regulatory T cells in induced tolerance to experimental autoimmune thyroiditis. Cell Immunol 2003;226:20–9.
25. Huang W, Kukes GD. Hashimoto's thyroiditis: an organ-specific autoimmune disease—pathogenesis and recent developments. Lab Invest 1999;79:1175–80.
26. Canonica GW, Cosulich ME, Croci R, et al. Thyroglobulin-induced T-cell *in vitro* proliferation in Hashimoto's thyroiditis: identification of the responsive subset and effect of monoclonal antibodies directed to Ia antigens. Clin Immunol Immunopathol 1984;32:132–41.
27. Kong YM, Lomo LC, Motte RW, et al. HLA-DRB1 polymorphism determines susceptibility to autoimmune thyroiditis in transgenic mice: definitive association with HLA-DRB1*0301 (DR3) gene. J Exp Med 1996;184: 1167–72.
28. Vladutiu AO, Rose NR. Autoimmune murine thyroiditis: relation to histocompatibility (H-2) type. Science 1971;174:1137–9.
29. Esquivel PS, Rose NR, Kong YM. Induction of autoimmunity in good and poor responder mice with mouse thyroglobulin and lipopolysaccharide. J Exp Med 1977;145:1250–63.
30. ElRehewy M, Kong YM, Giraldo AA, Rose NR. Syngeneic thyroglobulin is immunogenic in good responder mice. Eur J Immunol 1981;11:146–51.
31. Kong YM, Okayasu I, Giraldo AA, et al. Tolerance to thyroglobulin by activating suppressor mechanisms. Ann N Y Acad Sci 1982;392:191–209.
32. Mahoney KH, Miller BE, Heppner GH. FACS quantitation of leucine aminopeptidase and acid phosphatase on tumor associated macrophages from metastatic and nonmetastatic mouse mammary tumors. J Leukocyte Biol 1985;38:573–85.
33. Rovero S, Amici A, Di Carlo E, et al. Inhibition of carcinogenesis by DNA vaccination. J Immunol 2000; 165:5133–42.
34. Boggio K, Nicoletti G, Di Carlo E, et al. Interleukin 12-mediated prevention of spontaneous mammary adenocarcinomas in two lines of Her-2/neu transgenic mice. J Exp Med 1998;188:589–96.
35. Piechocki MP, Pilon S, Wei WZ. Quantitative measurement of anti-ErbB-2 antibody by flow cytometry and ELISA. J Immunol Methods 2002;259:33–42.
36. Kong YM. Experimental autoimmune thyroiditis in the mouse. In: Coligan JE, Kruisbeek AM, Margulies DH, Shevach EM, Strober W, editors. Current protocols in immunology. New York: John Wiley & Sons, Inc.; 1996. p. 15.7.1–15.7.16.
37. Kong YM, David CS, Giraldo AA, Elrehewy M, Rose NR. Regulation of autoimmune response to mouse thyroglobulin: influence of H-2D-end genes. J Immunol 1979;123:15–8.
38. Zhang W, Flynn JC, Kong YM. IL-12 prevents tolerance induction with mouse thyroglobulin by priming pathogenic T cells in experimental autoimmune thyroiditis: role of IFN-γ and the costimulatory molecules CD40L and CD28. Cell Immunol 2001;208:52–61.
39. Medina D, DeOme KB. Effects of various oncogenic agents on the tumor-producing capabilities of the D series of BALB/c mammary nodule outgrowth lines. J Nat Cancer Inst 1970;45:353–63.
40. Conaway DH, Giraldo AA, David CS, Kong YM. *In situ* kinetic analysis of thyroid lymphocyte infiltrate in mice developing experimental autoimmune thyroiditis. Clin Immunol Immunopathol 1989;53:346–53.
41. Curcio C, Di Carlo E, Clynes R, et al. Nonredundant roles of antibody, cytokines and perforin for the immune eradication of established Her-2/neu carcinomas. J Clin Invest 2003;111:1161–70.
42. Pilon SA, Kelly C, Wei WZ. Broadening of epitope recognition during immune rejection of ErbB-2-positive tumor prevents growth of ErbB-2-negative tumor. J Immunol 2003;170:1202–8.
43. Lindencrona JA, Preiss S, Kammertoens T, et al. CD4+ T cell-mediated HER-2/neu-specific tumor rejection in the absence of B cells. Int J Cancer 2004;109:259–64.

Downloaded from cancerres.aacrjournals.org on September 28, 2020. © 2005 American Association for Cancer Research.

AACR American Association for Cancer Research

Cancer Research

The Journal of Cancer Research (1916–1930) | The American Journal of Cancer (1931–1940)

Concurrent Induction of Antitumor Immunity and Autoimmune Thyroiditis in CD4 $^{+}$CD25^{+} Regulatory T Cell – Depleted Mice

Wei-Zen Wei, Jennifer B. Jacob, John F. Zielinski, et al.

Cancer Res 2005;65:8471-8478.

Updated version	Access the most recent version of this article at: http://cancerres.aacrjournals.org/content/65/18/8471
Supplementary Material	Access the most recent supplemental material at: http://cancerres.aacrjournals.org/content/suppl/2005/09/22/65.18.8471.DC1

Cited articles	This article cites 41 articles, 18 of which you can access for free at: http://cancerres.aacrjournals.org/content/65/18/8471.full#ref-list-1
Citing articles	This article has been cited by 16 HighWire-hosted articles. Access the articles at: http://cancerres.aacrjournals.org/content/65/18/8471.full#related-urls

E-mail alerts	Sign up to receive free email-alerts related to this article or journal.
Reprints and Subscriptions	To order reprints of this article or to subscribe to the journal, contact the AACR Publications Department at pubs@aacr.org.
Permissions	To request permission to re-use all or part of this article, use this link http://cancerres.aacrjournals.org/content/65/18/8471. Click on "Request Permissions" which will take you to the Copyright Clearance Center's (CCC) Rightslink site.

Downloaded from cancerres.aacrjournals.org on September 28, 2020. © 2005 American Association for Cancer Research.